

Structural Changes in Self-assembled Monolayers Initiated by Ultra-violet Light

*M. Hadi Zareie, * Jeffrey Barber and Andrew M. McDonagh**

Institute for Nanoscale Technology, University of Technology Sydney,

PO Box 123, Broadway NSW 2007, Australia.

hadi.zareie@uts.edu.au

RECEIVED DATE (to be automatically inserted after your manuscript is accepted if required according to the journal that you are submitting your paper to)

Abstract

Self-assembled monolayers of 2-anthracenethiol and 2-naphthalenethiol on gold(111) were irradiated with low-power UV light. Scanning tunnelling microscope images recorded in situ show unusual structural changes. In the case of 2-anthracenethiol, structures measuring 4-7 nm wide and 30-40 nm in length are formed. Images taken ten minutes after irradiation ceased show further surface reorganisation. With 2-naphthalenethiol SAMs, smaller structures form upon irradiation, which subsequently revert to resemble the original structure after time.

KEYWORDS (Word Style “BG_Keywords”). If you are submitting your paper to a journal that requires keywords, provide significant keywords to aid the reader in literature retrieval.

Introduction

There is significant interest in the interaction of UV light with self-assembled monolayers (SAMs) of thiulates and other molecules on gold surfaces. Irradiation with UV light can induce photodimerization in suitable molecular layers¹⁻⁴ but can also oxidize surface-bound thiols⁵⁻⁸ with the possible application of these processes in the rapidly expanding area of nanolithography.

Recently, Wan et al¹ presented data suggesting that 365 nm UV light initiated a dimerization reaction of a 4-amyloxycinnamic acid SAM on a gold surface. The reversible dimerization of pendent anthracene groups attached via C₁₀ chains in thiol-bound SAMs on gold has also been demonstrated.²

Detailed investigations into the mechanism of oxidation of surface-bound molecules have recently been published.^{9,10} It was suggested that using 254 nm light, electrons in the gold substrate may be excited and that these “hot” electrons subsequently initiate oxidation. Light from mercury arc lamps has also been shown to oxidize alkanethiols on gold substrates with the formation of ozone as a possible mechanism.^{11,12} In each of these cases, clarification of the mechanism is still an issue.

In the current work, the well-documented, reversible anthracene dimerisation reaction¹³ was investigated to ascertain if light-induced structural changes (and subsequent changes to the molecular conductivity) could be utilized to form molecular switches with anthracene units bound directly to a gold surface. This is shown schematically in the Figure 1. A SAM is probed using a scanning tunneling

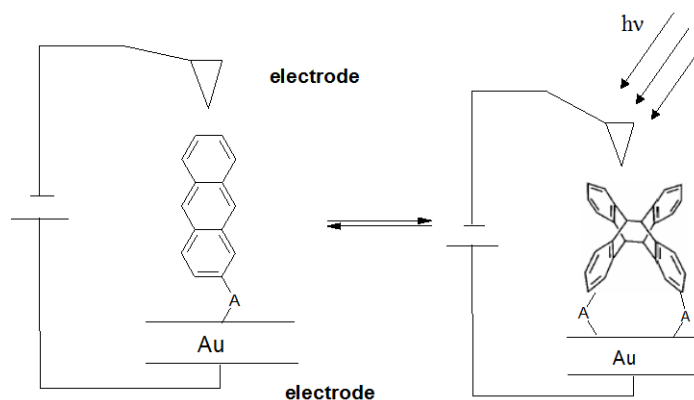


Figure 1. Schematic representation of a molecular switch based on the photodimerization reaction of anthracene. The circuit represents the probe and contact of a scanning tunneling microscope.

microscope (STM) while irradiating the surface with light of an appropriate wavelength. In Figure 1, the fully conjugated anthracene unit is attached to a gold surface by an appropriate anchoring group, A, and may undergo dimerization with a neighboring molecule upon irradiation to form a dimer that is not fully conjugated. In this work, we use thiol (SH) as an anchoring group, A. Recently, Witte et al¹⁴ reported that 2-anthracenethiol (Figure 2) forms SAMs that are stable under ambient conditions.

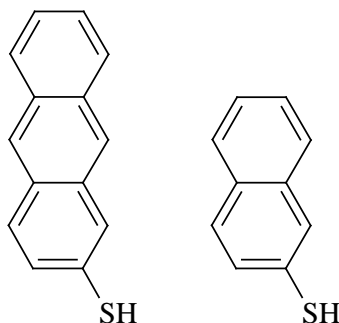


Figure 2. Compounds investigated in this work; 2-Anthracenethiol (left), and 2-Naphthalenethiol (right).

The absence of alkyl chains linking the anthracene unit to the anchoring thiol (in contrast to earlier work by Fox and Wooten²) is important because it has been shown¹⁵ that tunneling is the mechanism of conduction through thin organic layers. Therefore, increasing the distance between the switchable anthracene units and the gold surface would significantly diminish any observable changes in I/V characteristics upon dimerization.

This work investigates the UV-induced dimerization of anthracenethiol SAMs in light of the recent studies indicating that competing oxidation reactions may occur at these wavelengths.^{9,10} Thus, self-assembled monolayers of 2-anthracenethiol on gold(111) were irradiated with low-power 254 nm UV light ($\sim 1.6 \text{ mW/cm}^2$) and scanning tunneling microscope (STM) images were recorded. We present here STM images and data showing in situ observations of unusual structural changes in these SAMs

initiated by exposure to UV light. We also present STM data for SAMs of 2-naphthalenethiol (Figure 2) for comparison.

Results and Discussion

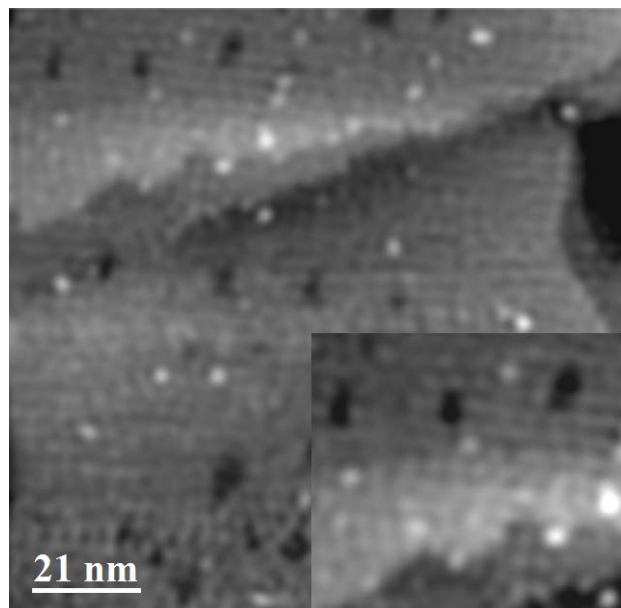


Figure 3. STM image of 2-anthracenethiol on gold (111). Bias voltage (V_b) = 1 V, tunneling current (I_t) = 1 nA. Inset shows a 30 x 25 nm magnified area.

SAMs of 2-anthracenethiol and 2-naphthalenethiol were prepared by literature procedures.¹⁶⁻¹⁸ Figure 3 shows STM images of a 2-anthracenethiol SAM. The monolayer forms with a dense coverage; steps associated with gold domain boundaries are also visible. A number of 2.4 Å deep vacancy islands are evident with the depth of these depressions correlating to the theoretical height of a single gold layer. The formation mechanism of these gold vacancy islands is described in detail in reference 19. These monatomic depressions are similar to those found in other thiol-bound SAMs on gold.^{19,20} Individual molecules are clearly visible in Figure 3 (inset). Line profile measurements using the image shown in Figure 3 indicate a molecular width of approximately 0.9 nm. This is in agreement with the calculated molecular width of 0.76 nm for a 2-anthracenethiol molecule oriented at an angle of 23.5° (based on data from reference 16) relative to the surface.

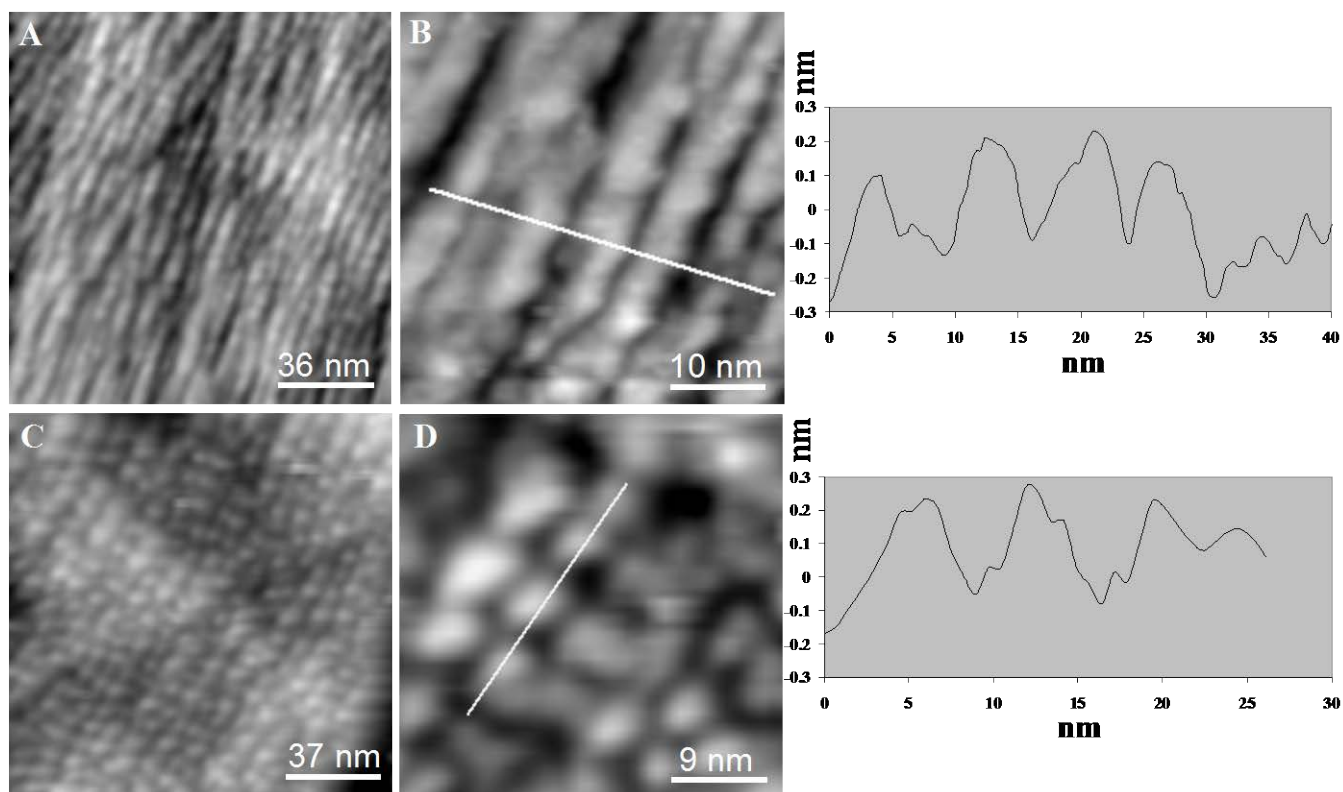


Figure 4. A: 2-anthracenethiol SAM immediately after exposure to 254 nm light. The features measure 4-7 nm wide, and 30-40 nm in length. B: Enlarged view of a region from A with the corresponding line profile region indicated. C: 2-anthracenethiol 10 minutes after ceasing UV irradiation. D: Enlarged view of a region from C with the corresponding line profile region indicated. $V_b = 1$ V, $I_t = 1$ nA.

The sample was irradiated with 254 nm light for ~1 minute. Importantly, the samples were not moved and the STM parameters remained fixed throughout the experiments so that a consistent set of images and data is obtained during the irradiation process for each SAM. Figure 4A and 4B shows STM images of the surface immediately after the lamp was turned off (images taken during irradiation were impaired due to electronic interference from the lamp). The SAM is significantly altered with structures measuring 4-7 nm wide and 30-40 nm in length appearing. The height measured by STM prior to irradiation is ~0.4 nm, which approximately doubles to ~0.8 nm measured after irradiation. We note that

heights of SAMs measured by STM are often less than the actual physical heights because both physical and electronic properties contribute to the STM height measurement.²¹

In contrast to Figure 3, no individual molecular features are visible within the bands. STM images of a sample taken after irradiation with 365 nm light showed no observable changes. To ascertain if the observed changes were a result of heating effects of the STM tip or some other UV-STM interaction, experiments were performed under identical conditions except that a bare gold substrate was probed. No changes to the surface were detected after UV irradiation. Furthermore, light-induced heating of STM tips has been shown to be a rapid and transient phenomenon²² and is unlikely to persist over timeframe of the current experiments. We conclude that the observed changes are due to a significant re-arrangement of the molecules comprising the SAM.

STM images taken 10 minutes after UV irradiation at 254 nm was ceased (Figure 4C and 4D) show further surface reorganisation to almost hemispherical structures with diameters of ~6 nm. The measured heights of the structures (~0.3 nm) are similar to the heights of the rope-like structures formed initially (Figure 4A and 4B).

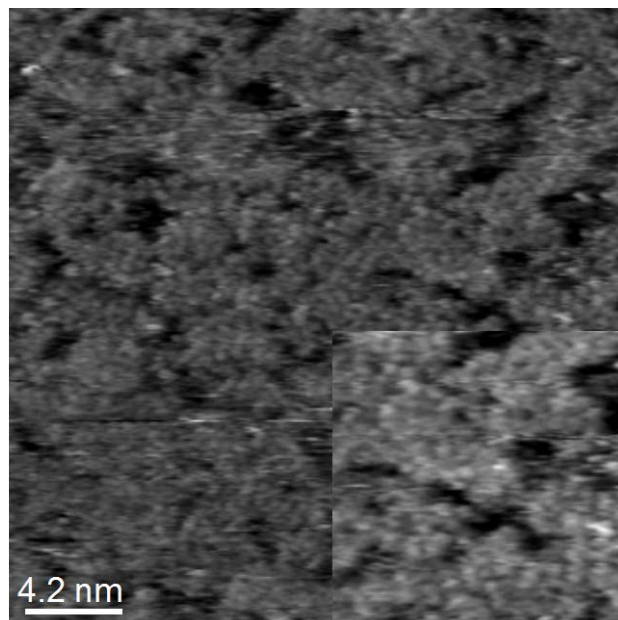


Figure 5. STM image of 2-naphthalenethiol SAM on gold(111). $V_b = 1$ V, $I_t = 1$ nA. Inset shows a 9 x 9 nm magnified area.

SAMs of 2-naphthalenethiol on Au(111) substrates were also prepared and imaged for comparison. This molecule has been previously reported¹⁸ to form stable SAMs that are not prone to oxidation. Figure 5 shows, to the best our knowledge, the first reported STM images of a 2-naphthalenethiol SAM. Individual molecules can be resolved with dimensions of $\sim 0.7 \times 0.25$ nm, in agreement with calculated molecular dimensions.

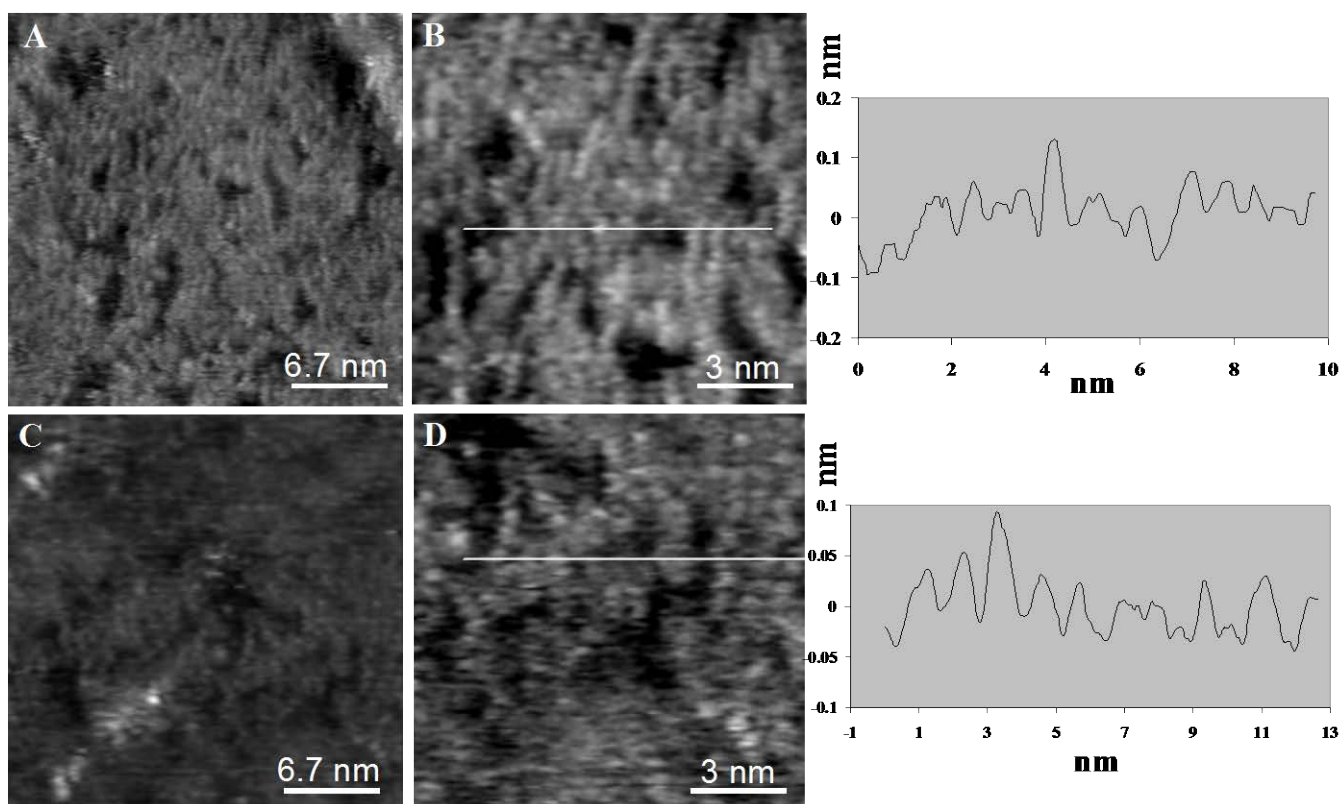


Figure 6. A: 2-Naphthalenethiol SAM immediately after UV irradiation. B: Enlarged view of a region from A with the corresponding line profile region indicated. C: 2-Naphthalenethiol SAM 10 minutes after ceasing irradiation. D: Enlarged view of a region from C with the corresponding line profile region indicated. All images, $V_b = 1$ V, $I_t = 1$ nA.

Figure 6A shows the same surface immediately after ~1 minute of exposure to 254 nm light. Chain-like structures appear with features ~0.7 nm wide and 1.0-1.5 nm in length. Figure 6C shows the surface 10 minutes after irradiation was ceased. The surface reorganizes in this time with features of ~0.7 x 0.3 nm observed, similar to those seen in the original image (Figure 5) although some chain-like structures remain. Clearly, the changes are different to those seen in the 2-anthracenethiol SAMs.

Given that photoinduced dimerization of naphthalene compounds is an extremely inefficient process,²³ we propose that the larger structures observed in the 2-naphthalenethiol SAMs after UV exposure may be attributed to interactions between thiol groups. This is entirely consistent with previous studies that show that disulfides in SAMs can be produced by UV irradiation,²⁴ and also that disulfide bonds may readily cleave to form thiolate monolayers on gold surfaces.²⁰ Interestingly, the dinaphthalene disulfide compound (obtained by formation of a disulfide bond between two naphthalenethiol molecules) has calculated dimensions similar to those of the features observed in Figure 6A (modelling shows the disulfide molecule to be 0.7 x 1.3 nm).

Because the UV-induced changes in the 2-naphthalenethiol SAMs are far less obvious than in the 2-anthracenethiol examples, x-ray photoelectron spectroscopy (XPS) experiments were conducted to investigate the possibility that changes were due to irreversible photo-induced surface oxidation processes.

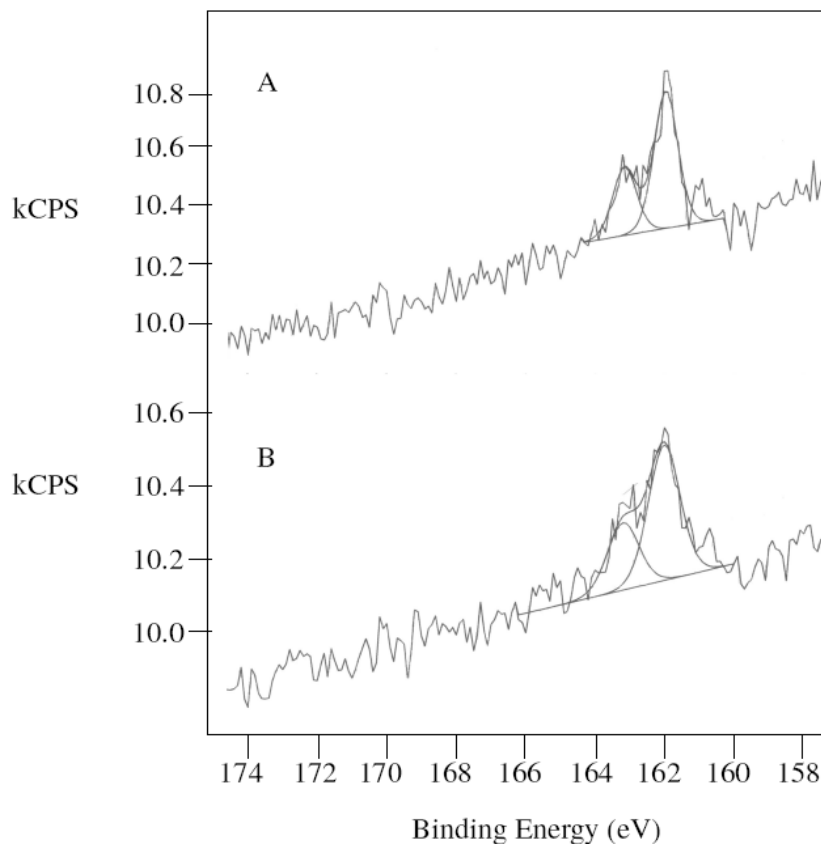


Figure 7. XPS spectra showing the S_{2p} region. A: 2-naphthalenethiol SAM before irradiation. B: 2-naphthalenethiol SAM after 40 minutes irradiation.

A freshly prepared SAM was analysed by XPS and then irradiated under identical conditions to those used in the STM experiments i.e., ambient atmosphere with the same light intensity. After one minute of irradiation, the sample was re-analysed and the procedure repeated with an irradiation period of 40 minutes. Figure 7 shows the S 2p regions of the XPS spectra of the freshly prepared sample, A, and the sample after 40 minutes irradiation, B. The curve-fitted spectra show S 2p doublets at 163.2 and 162.0 eV, consistent with sulfur atoms involved in a thiolate-gold bond. This binding energy is similar to those reported for a number of other aromatic thiol SAMs.¹⁶ Even after the 40-minute period of irradiation, the spectra are virtually identical. If surface-bound sulfur atoms were oxidized to species containing sulfur-bonded oxygen atoms, signals at higher binding energy would be expected. For example, Hutt and Leggett⁸ found that upon oxidation of alkanethiol SAMs, the S 2p signal shifts to a binding energy of

~167 eV. This is not the case in the current work. The C 1s region of the XPS spectrum contains a large peak at 284.2 eV assigned to the carbon atoms of the naphthalene ring. Also evident are smaller peaks at 288.7, 286.5, and 285.1 eV, which suggest that the deposited film has some carbon-containing contaminants,²⁵ evidenced also by a single peak in the O 1s region at 532.6 eV. No change in these features was detected upon irradiation. We conclude from the STM and XPS experiments that no irreversible processes occur upon irradiation of the 2-naphthalenethiol SAMs, and propose that if any oxidation of sulfur occurs, it is to a disulfide species that upon removal of the light source, reverts to the original monomeric thiolate species.

In contrast, dimerization of anthracene compounds may proceed readily upon irradiation. As a consequence, anthracene dimers as well as disulfides may form in this case. It may be concluded that the difference in behaviour of the 2-anthracenethiol SAM may be attributed to anthracene-anthracene interactions. We are currently investigating other anthracene-based SAMs in an attempt to further elucidate the mechanism of this unusual structure formation.

Conclusion

STM images of anthracene- and naphthalenethiol SAMs reveal unusual structural rearrangements upon irradiation with 254 nm UV light. In terms of our original goal of a light-activated molecular switch, we find that the use of the reversible anthracene dimerisation reaction initiated by UV light appears to be incompatible with 2-anthracenethiol SAMs. However, the larger than expected structures observed here may have applications in the area of nanopatterning. Importantly, the capability of STM to directly observe the effect of UV light on molecular structures has been demonstrated. This may be useful in future examinations of UV-induced processes in other SAM systems.

Experimental Section

The self-assembled monolayer structures on gold(111) were made by literature procedures.¹⁶⁻¹⁸ STM measurements were performed using either a Nanosurf Easyscan system or a DI Multimode under ambient conditions. STM tips have been prepared by mechanically cutting a 0.2 mm thick Pt/Ir (80/20) 0.2 mm wire. All images were acquired in a constant-current mode. Typical imaging conditions are bias

voltages of 1 V and a tunneling current of 1 nA. Images were acquired from three different samples for each SAM. No significant variation was observed between the different samples for a given SAM. Images were manipulated with the Scanning Probe Image Processor (SPIP) software. Dimensions of features in the images were taken by a combination of peak-to-peak measurements from line profiles and measured profile lengths.

XPS data were acquired using a ESCALAB220i-XL X-ray Photoelectron Spectrometer. The incident radiation was monochromatic Al K-alpha X-rays at 240W (10 kV, 24 ma) with a spot size of 1 mm diameter. Survey (wide) scans were taken at an analyzer pass energy of 100 eV and narrow high resolution scans at 20eV.

A Minerallight Multiband UV lamp (Pathtech Model UVGL-55) was used for UV irradiation at either 254 nm or 365 nm wavelengths. The lamp was placed 10 cm above the sample to give an intensity of 1.6 mW/cm² at the surface. Geometry optimized molecular dimensions were calculated using Accelrys MS Modelling with VAMP.

Acknowledgement The authors thank Profs M. B. Cortie and M.J. Ford for helpful discussions and suggestions, Dr Bill Gong from the School of Chemistry at the University of New South Wales for XPS experiments, and the Australian Research Council for financial support.

References

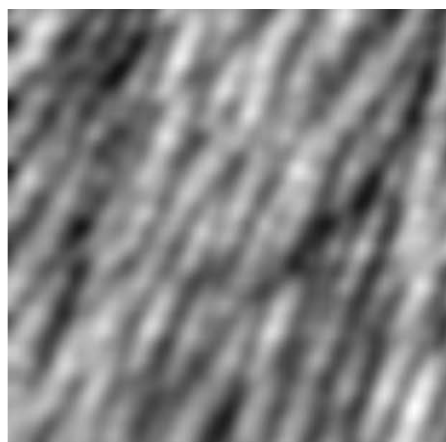
1. Xu, L-P.; Yan, C-J.; Wan, L-J.; Jiang, S-J.; Liu, M-H. *J. Phys. Chem. B.* **2005**, *109*, 14773.
2. Fox, M. A.; Wooten, M. D. *Langmuir* **1997**, *13*, 7099.
3. Vanoppen, P.; Grim, P. C. M.; Ruecker, M.; De Feyter, S.; Moessner, G.; Valiyaveetil, S.; Müllen, K.; De Schryver, F. C. *J. Phys. Chem.* **1996**, *100*, 19636.
4. Abdel-Mottaleb, M. M. S.; de Feyter, S.; Gesquiere, A.; Sieffert, M.; Klapper, M.; Müllen, K.; de Schryver, F. C. *Nano Lett.* 2001, *1*, 353.
5. Huang, J.; Hemminger, J. C. *J. Am. Chem. Soc.* 1993, *115*, 3342.
6. Ishida, T.; Sano, M.; Fukushima, H.; Ishida, M.; Sasaki, S. *Langmuir* 2002, *18*, 10496.
7. Rieley, H.; Kendall, G. K.; Zemicael, F. W.; Smith, T. L.; Yang, S. *Langmuir* 1998, *14*, 5147.
8. Hutt, D. A.; Leggett, G. J. *J. Phys. Chem.* 1996, *100*, 6657.
9. Brewer, N. J.; Janusz, S.; Critchely, K.; Evans, S. D.; Leggett, G. J. *J. Phys. Chem. B.* 2005, *109*, 11247.
10. Brewer, N. J.; Rawsterne, R. E.; Kothari, S.; Leggett, G. J. *J. Am. Chem. Soc.* **2001**, *123*, 4089.
11. Norrod, K. L. Rowlen, K. L. *J. Am. Chem. Soc.* **1998**, *120*, 2656.
12. Zhang, Y.; Terrill, R. H.; Bohn, P. W. *Chem. Mater.* **1999**, *11*, 2191.
13. Bousa-Laurent, H.; Castellan, A.; Desvergne, J-P.; Lapouyade, R. *Chem. Soc. Rev.* **2000**, *29*, 43.
14. Käfer, D.; Witte, G.; Cyganik, P.; Terfort, A.; Wöll, C. *J. Am. Chem. Soc.* **2006**, *128*, 1723.
15. Maisch, S.; Buckel, F.; Effenberger, F.; *J. Am. Chem. Soc.* **2005**, *127*, 17315.

16. Frey, S.; Stadler, V.; Heister, K.; Eck, W.; Zharnikov, M.; Grunze, M. *Langmuir* **2001**, *17*, 2408.
17. Scharf, J.; Strehblow, H.; Zeysing, B.; Terfort, A. *J. Solid State Electrochem.* **2001**, *5*, 396.
18. Kolega, R. R.; Schlenoff, J. B. *Langmuir* 1998, *14*, 5469.
19. Yang, G.; Liu, G.-Y. *J. Phys. Chem. B.* **2003**, *107*, 8746.
20. Love, J. C.; Estroff, L. A.; Kriebel, J. K.; Nuzzo, R. G.; Whitesides, G. M. *Chem. Rev.* **2005**, *105*, 1103.
21. Bumm, L. A.; Arnold, J. J.; Dunbar, T. D.; Allara, D. L.; Weiss, P. S. *J. Phys. Chem. B* **1999**, *103*, 8122.
22. Grafström, S.; Schuller, P.; Kowalski, J.; Neumann, R. *J. Appl. Phys.* **1998**, *83*, 3453.
23. Albini, A.; Fasani, E.; Gamba, A. *J. Photochem. Photobiol. A.* **1988**, *41*, 215.
24. Kohli, P.; Taylor, K. K.; Harris, J. J.; Blanchard, G. J. *J. Am. Chem. Soc.* **1998**, *120*, 11962.
25. Ishida, T.; Tsuneda, S.; Nishida, N.; Hara, M.; Sasabe, H.; Knoll, W. *Langmuir* **1997**, *13*, 4638.

Table of Contents Image:



UV light
(254 nm) →



2-Anthracenethiol SAM